DIFFRACTION EFFECTS IN THE COHERENT TRANSITION RADIATION BUNCH LENGTH DIAGNOSTICS *

G. Kazakevich, V. Lebedev, S. Nagaitsev,
FNAL, P.O. Box 500, Batavia, Illinois 60510, USA

Abstract

Diffraction effects in the Coherent Transition Radiation (CTR) bunch length diagnostics are considered for the A0 Photoinjector and the New Muon Laboratory (NML) injection module. The effects can cause a noticeable distortion of the measured CTR spectra depending on the experimental setup and the bunch parameters and resulting in errors of the bunch length measurenents. Presented calculations show possible systematic errors in the bunch length in measurements based on the CTR spectra at A0 Photo injector and the NML injection module.

INTRODUCTION

Application of the CTR diagnostics for the sub-picoseconds bunch length measurements was proposed more than 10 years ago and a number of articles have been devoted to the experiments in this field. The diagnostics employing the Transition Radiation (TR), [1], are based on the measurements of the CTR spectra to restore the bunch length through the Fourier transform. In this article we consider low-frequency TR range where the coherent part of the spectrum dominates and the wavelengths are about the bunch length. For such low-frequency harmonics one should not neglect the diffraction effects in the coherent radiation diagnostics, [2, 3, 4]. They can strongly distort the measured CTR spectra depending on the beam energy and the experimental setup. We discuss computations of the CTR diffraction effects in application to the measurements at A0 Photoinjector, [5], and the NML injection module [6].

ELECTRIC FIELD OF THE TR AND CTR

Most experimental techniques using CTR spectra for the bunch length measurements employ backward TR generated at 45^0 incidences of electrons on the mirror-quality metallic screen. This radiation has a spectral density practically similar to the one for the backward TR at the normal incidence. For simplicity we consider only this case. To estimate the diffraction effects we assume a finite radius *a* of the TR screen. Finite size of vacuum chamber we do not consider for sake of simplicity though it also affects the bunch longitudinal profile. We also assume that the screen is located at the origin of the cylindrical frame η: $(\rho, \phi, z = 0)$, and the *z* axis is directed along the momentum of the electron beam. The observation point is displaced at a distance $D>>a$ along *z*.

A derivation of required formulae generally follows to Ref. [4], where the consideration is based on the virtual-photon method applicable for ultra relativistic electrons.

The Fourier harmonic of the radial electric field for the incident single electron is expressed as, [7, 4]:

$$\widetilde{E}_r(\omega,\rho) = \frac{-e\omega}{(2\pi)^{3/2}\varepsilon_0\beta^2c^2\gamma} K_1\left(\frac{\omega\rho}{\beta c\gamma}\right), \quad (1)$$

where: ε_0 is the permittivity of vacuum, $K_1(u)$ is the second kind modified Bessel function. We assume that the virtual photon constituting the electron self-field is converted into the real TR photon. Considering continuity of the normal components of the electric induction and tangential components of the electric field of the virtual and real (reflected) photons, [8], one can conclude that the amplitudes of the radial components of virtual and real photons are same, i.e. the electric field of an ultra relativistic electron is almost completely reflected from metal screen. The small element of the TR screen with coordinates $(\rho,\phi,0)$ gives following contribution to the field (this field is also radial) in the point of observation *(x,0,D)* :

$$d\widetilde{E}_x(x,0,D,\omega) = \frac{-i\omega}{2\pi c}\widetilde{E}_r(\omega,\rho)\cos\phi\frac{e^{\frac{i\omega R'}{c}}}{R'}\rho d\rho d\phi\,. \quad (2)$$

Here: R' is a distance between the points $(\rho,\phi,0)$ and (*x*,0,*D*),

$$R' = \sqrt{D^2+(x-\rho\cos\phi)^2+(\rho\sin\phi)^2} \approx R - \frac{x\rho\cos\phi}{R} + \frac{\rho^2}{2R}, \quad (3)$$

and: $R = \sqrt{D^2+x^2}$. Substitution (1) and (3) into (2) with $x/R = \sin\theta$ and integration over the TR screen area yields for the electric field in the point (*x*,0,*D*):

$$\widetilde{E}_x(x,0,D,\omega) \approx \frac{ie\omega^2}{(2\pi)^{5/2}\varepsilon_0\beta^2c^3\gamma}\cdot\frac{e^{\frac{i\omega R}{c}}}{R}\times \int_0^a\left[\int_0^{2\pi}K_1\left(\frac{\omega\rho}{\beta c\gamma}\right)\cos\phi\cdot e^{\frac{-i\omega\rho\sin\theta\cos\phi}{c}}d\phi\right]\cdot e^{\frac{i\omega\rho^2}{2cR}}\rho d\rho\,. \quad (4)$$

In this expression the integration over angle ϕ gives the first kind Bessel function $J_1(z)$:

$$\int_0^{2\pi} e^{\frac{-i\omega\rho\sin\theta\cdot\cos\phi}{c}}\cos\phi\cdot d\phi = -i2\pi\cdot J_1\left(\frac{\omega\rho\sin\theta}{c}\right),$$

That yields:

*Work supported by Fermi Research Alliance LLC. Under DE-AC02-07CH11359 with the U.S. DOE
#kazakevi@fnal.gov

$$\widetilde{E}_x(x,0,D,\omega) \approx \frac{e\omega^2}{(2\pi)^{3/2}\varepsilon_0\beta^2c^3\gamma}\cdot\frac{e^{\frac{i\omega R}{c}}}{R}\times$$

$$\int_0^a J_1\left(\frac{\omega\rho\sin\theta}{c}\right)K_1\left(\frac{\omega\rho}{\beta c\gamma}\right)\cdot e^{\frac{i\omega\rho^2}{2cR}}\rho d\rho\,. \qquad (5)$$

The flow of the TR energy in the observation plane is: $S_z=(1/2\mu_0)\widetilde{E}_x\widetilde{B}_y^*$, where the magnetic field Fourier component is: $\widetilde{B}(\omega)=\widetilde{E}(\omega)/c$, and μ_0 is the permeability of vacuum. Total energy per unit area radiated through element $ds=dx\cdot dy$ is [8]:

$$\frac{d^2U}{d\omega d\Omega} = I(\omega,\theta) = 2\varepsilon_0 cR^2\left|\widetilde{E}_x(\omega,\theta)\right|^2, \qquad (6)$$

where: $ds = R^2 d\Omega$.

Eqs. (5) and (6) include both: the Fraunhofer diffraction in far-field zone and the Fresnel diffraction in the near-field zone. The inequalities: $a < \gamma\lambda$ and $D < \gamma^2\lambda$ (λ is the wavelength of the TR harmonic), [9], give a region where the Ginzburg-Frank formula [1] has to be corrected for the diffraction. The Fraunhofer diffraction approximation considering finite size of the TR screen neglects the third term in Eq. (3); while the Fresnel diffraction approximation neglects the second term in Eq. (3). For the far-field measurements one can omit the Fresnel diffraction effect.

In ultra relativistic case and $a\to\infty$ results obtained from Eq. (5) for far-field zone coincide with those obtained with Ginzburg-Frank formula, therefore, for TR in the optical wavelength range at the electron energy of tens-hundreds MeV the diffraction effects are negligible and there is no need to use the above expressions to calculate the angular distribution of the radiation, however at the TR wavelength in the sub millimeter-millimeter range the diffraction effects become noticeable.

Using Eq. (5), derived for point like charge, one can obtain an expression for finite size bunch with charge Ne using the following method. First, we consider Fourier spectrum of the current of point-like bunch moving with velocity of $\vec{v}$ along z axis. The corresponding Fourier harmonics are:

$$j_{k\omega} = \int_{-\infty}^{\infty} Nev\delta(r-vt)e^{i(\omega t-kr)}\frac{dtdr}{(2\pi)^4} = \frac{Nev\cdot\delta\left(\omega-(\vec{k}\vec{v})\right)}{(2\pi)^4}.$$

Then we consider Fourier spectrum for a bunch with Gaussian distribution along z axis and infinitely small transverse sizes:

$$j_{k\omega} = \frac{Nev}{(2\pi)^4\sqrt{2\pi}\sigma}\int_{-\infty}^{\infty} e^{-\frac{(z-vt)^2}{2\sigma^2}}\cdot e^{i(\omega t-\vec{k}\vec{r})}dtdr^3.$$

Introducing new variable: $z`=z-vt$ and taking into account that: $\left(\frac{(z`)^2}{2\sigma^2}+ik(z`)\right)=\frac{\left(z`-i\sigma^2k\right)^2+\sigma^4k^2}{2\sigma^2}$,

$$\int_{-\infty}^{\infty} e^{-2i\cdot\pi\cdot kx}dk=\delta(x),\ \int_{-\infty}^{\infty} e^{-x^2}dx=\sqrt{\pi}=\int_{-\infty}^{\infty} e^{-(x+ai)^2}dx,$$

one can write:

$$j_{k\omega} = \frac{Nev}{(2\pi)^4}\delta(\omega-kv_0)\exp\left(\frac{-\sigma^2k_z^2}{2}\right).$$

Here: k_z is projection of $\vec{k}$ on z axis. For small angles $k_z^2 \approx k^2(1-\theta^2)$, this results in:

$$j_{k\omega} = \frac{Nev}{(2\pi)^4}\delta(\omega-k_zv_0)\exp\left(\frac{-\sigma^2k^2(1-\theta^2)}{2}\right).$$

Comparing this expression with the Fourier harmonics of the point-like bunch current one obtains the term describing TR for finite size bunch. The term in a frequency domain is expressed as:

$$S(\omega) = N\exp\left(-\omega^2(1-\theta^2)/2\sigma_\omega^2\right). \qquad (8)$$

Thus in the case of longitudinal Gaussian distribution Eqs. (5) and (7) have to be supplemented by term $S(\omega)$. For $\theta<<1$ it results in,

$$S(\omega) \approx N\exp\left(-\omega^2/2\sigma_\omega^2\right).$$

Corresponding form-factor for spectral density of coherent radiation of the N electrons is:

$$F(\omega) = \left(S(\omega)\right)^2. \qquad (9)$$

That yields the total CTR spectral power within the angle θ_0 to be equal to:

$$I_{cd}(\omega) = 2\pi\int_0^{\theta_0} F(\omega)\cdot I(\omega,\theta)\sin\theta\cdot d\theta\,. \qquad (10)$$

Using this spectral power one can determine the bunch length through the inverse Fourier transformation.

DIFFRACTION EFFECTS IN THE SINGLE ELECTRON TR

Angular distributions of the backward TR generated by passage of single electron through the TR screen were computed using Eqs. (5), (6). The results for the wavelengths, λ, of 1, 0.3, 0.1 mm and the electron energies of 15 and 40 MeV are plotted in Figs. 1, 2.

The TR screen radius, a=12.5 mm of existing real setup and the distances R =250 mm and R >>250 mm (far field zone) were used in the computations.

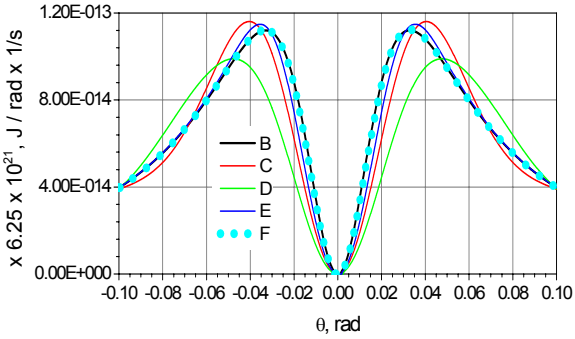

Fig. 1. Angular distribution of the backward TR for different wavelengths and 15 MeV electrons. C- λ=1 mm,

far-field zone; D- λ=1 mm, R=250 mm; E- λ=0.3 mm, R=250 mm; F- λ=0.1 mm, R=250 mm. Curve B was computed using Ginzburg-Frank formula.

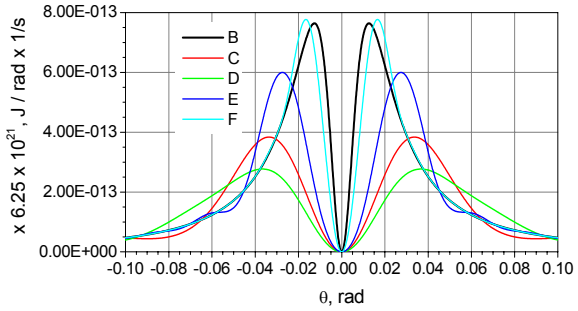

Fig. 2. Angular distribution of the backward TR for different wavelengths and 40 MeV electrons. C- λ=1 mm, far-field zone; D- λ=1 mm, R=250 mm; E- λ=0.3 mm, R=250 mm; F- λ=0.1 mm, R=250 mm. Curve B was computed using Ginzburg-Frank formula.

For comparison the angular distributions of the backward TR calculated using the Ginzburg-Frank formula (where the spectral density does not depend on the frequency in a wide range) are also shown in these figures.

The plots show that the diffraction effects caused by finite TR screen size noticeably change the angular distribution of the TR especially for low frequencies. Computation of the angular distribution using Eq. (5) and (6) for the TR screen radius $a > \gamma\lambda$ and detection of the TR in the far-field zone results in excellent agreement with calculation using the Ginzburg-Frank formula; but for $a < \gamma\lambda$ and/or detection of the TR at $D < \gamma^2\lambda$ a noticeable difference appears. An increase of the energy of electrons magnifies the difference for long-wavelength TR due to diffraction effects, in spite of the narrower angular distribution of the TR at higher energy. The diffraction phenomenon becomes apparent in a broadening of the TR angular distribution for longer waves.

Since the CTR exists in long-wave part of spectrum, the broadening in the angular distribution causes a distortion of the measured CTR spectra in a real experimental setup. This additionally complicates determination of the bunch length in methods employing the CTR techniques.

DIFFRACTION EFFECTS IN THE CTR SPECTRA

The spectra for the Gaussian distributions with rms bunch duration of σ_t = 1.5 ps, 0.5 ps. and 0.15 ps are presented by Gaussians with rms frequency width σ_f = 0.107 THz, 0.322 THz and 1.07 THz, respectively.

The CTR spectra corresponding to real setups were calculated using Eqs. (5), (6) and (10) for θ_0 = 0.05 rad. and 0.1 rad. Dependences of the spectra on the σ_t of the bunch, beam energy and setup condition are shown in Figs. 3-5.

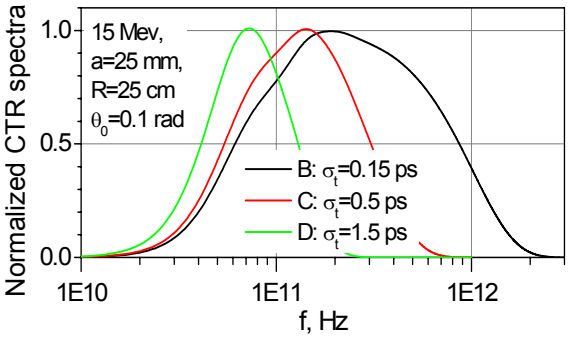

Fig. 3. Calculated normalized CTR spectra for 15 MeV for different σ_t at a=25 mm, θ_0=0.1 rad.

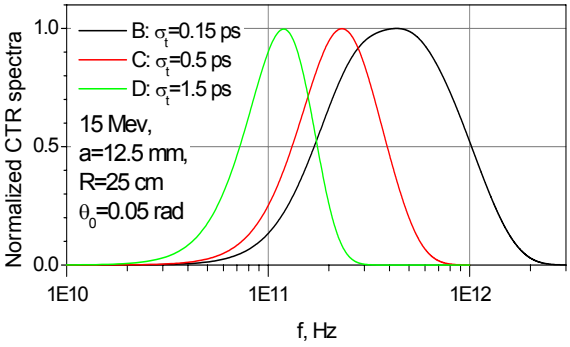

Fig. 4. Calculated normalized CTR spectra for 15 MeV for different σ_t at a=12.5 mm, θ_0=0.05 rad.

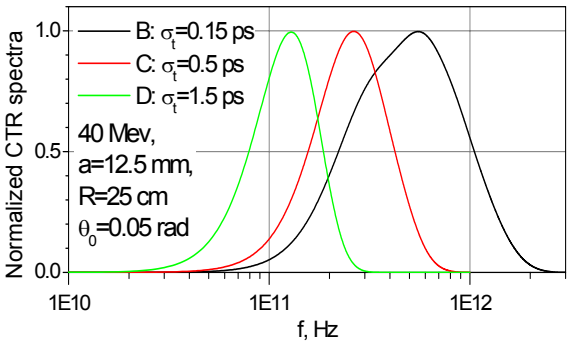

Fig. 5. Calculated normalized CTR spectra for 40 MeV for different σ_t at a=12.5 mm, θ_0=0.05 rad.

The plotted curves show significant variation of the CTR spectra with parameters of the experiment because of diffraction effects. The effects noticeably shift low frequency boundary of the CTR spectra to higher frequencies at limited size of the TR screen and limited detector acceptance. In fact these phenomena lead to the "shortening" of the electron bunch length if it is computed using the inverse Fourier transform. Corresponding results are shown in Fig. 6 for different σ_t values at 15 MeV, a=12.5 mm and θ_0=0.05 rad.

We introduce the dimensionless relative σ_r as the ratio of the computed (using inverse Fourier transform of the

CTR spectra) σ_t value to the real σ_t value of the bunch with Gaussian longitudinal distribution. It is plotted in Fig. 7 for different beam energies and setup parameters.

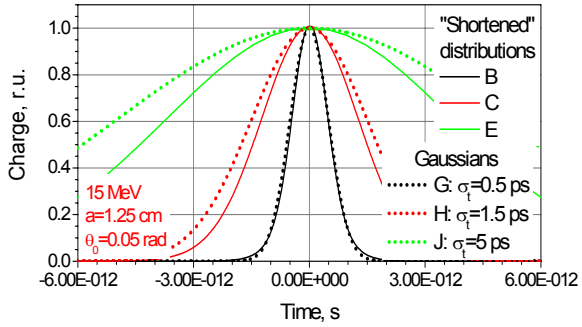

Fig. 6. "Shortening" in the bunch duration caused by diffraction. Curves *B, C, E* correspond to σ_t=0.5, 1.5, 5 ps, respectively.

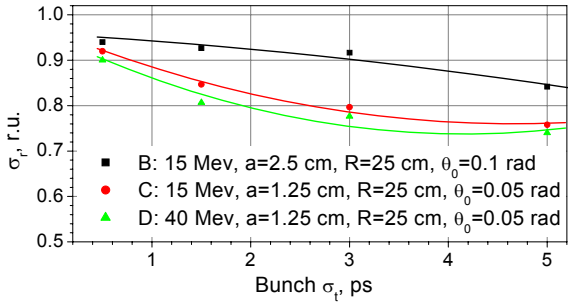

Fig. 7. Bunch "shortening" caused by diffraction effects for different bunch durations, setup geometries and beam energy.

Presented plots evaluate systematic errors in the bunch length caused by diffraction, if distortion of CTR spectra is unaccounted. The effects become noticeable at low frequencies (longer bunch length) and they are caused by both: the finite size of the TR screen (the Fraunhofer diffraction) and the finite distance to the detecting device at finite acceptance of the detecting device (the Fresnel diffraction) as well.

Note that the same systematic errors are inherent to all methods based on the measurements of the coherent radiation, including methods utilizing non-linear optical crystals.

The ordinary experimental setup employing the TR screen of 25 mm in diameter at detection of the CTR in the range of ± 0.05 rad. gives relative systematic error in the bunch length of ≈ 10% at the bunch length of 0.5 mm and at the electron beam energy of 15 MeV. At longer bunch the diffraction more distorts the CTR spectra and systematic error in the bunch length should be bigger if the CTR diagnostics are used. For the bunch length of ≈ 3 mm the relative systematic error is increased up to ~24% for Gaussian longitudinal bunch profile. Higher energy of the electrons causes bigger distortion of the CTR spectra and, correspondingly, bigger systematic error in the bunch length determination. Figure 8 presents systematic errors of the bunch length calculations caused by diffraction for Gaussian longitudinal bunch profiles.

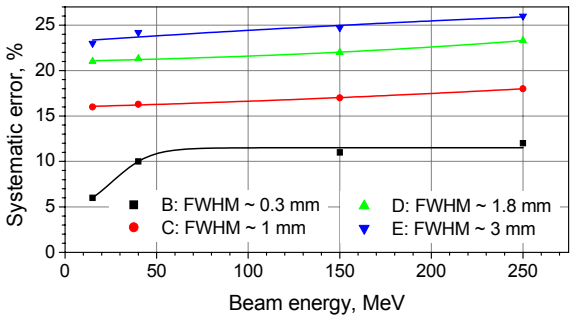

Fig. 8. Systematic errors caused by diffraction effects in finding of the bunch length based on the CTR techniques for different beam energies.

The presented plots were calculated at *a =1.25 cm*, *R = 25 cm*, θ_0 *=0.05* rad. As follows from Fig. 8 those setup parameters provide systematic errors ≤ 5% for the bunch length ≤ 0.3 mm at the beam energy up to 15 MeV and ~ 12% at the beam energy of 250 MeV. Increase of the bunch length causes a stronger distortion of the result. Increase of the beam energy also amplifies a distortion of the result.

SUMMARY

If uncounted, the diffraction distortions of the CTR spectra result in systematic errors of the bunch length measurements depending on the setup and the bunch parameters. The diffraction corrections should be considered in the planned experiments at the A0 Photoinjector and the NML injection module.

REFERENCES

[1] V.L Ginzburg and I.M. Frank, J. Exp. and Theoret. Phys., Vol. 16, pp. 15-21, 1946

[2] M. Castellano and V.A. Verzilov, PRST-AB V1, 062801, (1998)

[3] M. Castellano et al., NIM A 435, (1999), 297-307

[4] S. Casalbuoni et al., TESLA Report 2005-15

[5] J.P. Carneiro et al., "First Results of the Fermilab High-Brightness RF Photoinjector", Proc. of the 1999 PAC Conference, NY, 1999, pp. 2027-2029

[6] M. Church et al., "Plans for a 750 MeV Electron Beam Test Facility at Fermilab" PAC 2007 report, PAC Conference, Albuquerque, New Mexico, 2007

[7] J.D. Jackson, Classical Electrodynamics, J. Wiley & Sons, 1998

[8] L.D. Landau and E.M. Lifshitz, Electrodynamics of Continuous Media, Pergamon, New York, 1960

[9] V.A. Lebedev, NIM A 372, (1996), 344-348